scientific reports

OPEN

Influence of lateral single jets for thermal protection of reentry nose cone with multi-row disk spike at hypersonic flow: computational study

Yunbin Shi[1]✉, Qiong Cheng[1], As'ad Alizadeh[2], Hongbo Yan[3], Gautam Choubey[4], K. Fallah[5]✉ & Mahmoud Shamsborhan[6]

The main challenge for the advancement of current high-speed automotives is aerodynamic heating. In this study, the application of lateral jet for thermal protection of the high-speed automotives is extensively studied. The simulation of the lateral coolant jet is done via Computational fluid dynamic at high-velocity condition. Finding optimum jet configuration for reduction of the aerodynamic heating is the main goal of this research. Two different coolant jets (Helium and Carbon dioxide) are investigated as coolant jet and flow study and fuel penetration mechanism are fully presented. In addition, the thermal load on the main body of nose cone is compared for different configurations. Our results specify that the injection of lateral jet near the tip of spike is effective for thermal protection of main body via deflection of bow shock. Also, Carbon dioxide jet with lower diffusivity is more effective for the protection of forebody with multi-row disk from sever aerodynamic heating.

In the aerospace and automotive context, Aerodynamic heating is known as the process of heating near the solid body due to change of the hypersonic/supersonic flow into energy term[1,2]. Although it seems that the transformation of momentum into thermal energy is simple process, its impacts on the flow are highly complicated[3–5]. The process of aerodynamic heating mainly happens near the nose cone of high-speed automotives. This process is highly significant for these high-speed automotives and it influences on the burning of the nose cone because of the splendid heating[6–9]. In addition, aerodynamic heating results in the noise for transmission of digital signal. These disadvantageous of aerodynamic heating have motivated the aerospace and automotive engineers to manage this process[10–12].

There are several techniques for protection of the nose cone from aerodynamic heating. The main challenge for managing of aerodynamic heating is drag force[13–15]. In fact, drag force level should be kept in the recommended techniques. Three main techniques of mechanical, fluidic and energy devices have been investigated and examined in the previous works[16–19]. In these techniques, spike, coolant jet and energy source are used, respectively, to avoid attachment of the free stream to the main body. These techniques could efficiently reduce the temperature of the main stream after receiving to the main body[20–22]. However, the main challenge for these techniques is high drag force and this is the topic of the researchers to resolve this problem in this field[23,24].

Among these methods, the main conventional technique for reduction of high heat load near the nose cone is spike[25–28]. Spike is known as the long thin rod located at tip of nose cone to deflect the main supersonic flow from main nose cone[29,30]. The usage of spike as a practical method is due to its simplicity[31,32]. Besides, the drag force is reduced in this technique since the supersonic air stream is bifurcated by spike. The shape of spike tip and length of spike is known as two effective factors on the performance of this technique. Previous researches[33–37] showed that the cooling performance of this technique is not acceptable as drag force although limited thermal load

[1]Geely Automotive Institute, Hangzhou Vocational & Technical College, Hangzhou 310018, China. [2]Department of Civil Engineering, College of Engineering, Cihan University-Erbil, Erbīl, Iraq. [3]Geely Automobile Research Institute (Ningbo) Co., Ltd., Ningbo 315336, China. [4]Department of Mechanical & Aerospace Engineering, Institute of Infrastructure Technology Research and Management (IITRAM), Ahmedabad, Gujarat 380026, India. [5]Department of Mechanical Engineering, Semnan University, Semnan, Iran. [6]Department of Mechanical Engineering, College of Engineering, University of Zakho, Zakho, Iraq. ✉email: shiyunbin578@sina.com; kfallah1@outlook.com

reduction is reported by the application of the spike. Therefore, investigations have focused on new techniques which could compensate this deficiency of mechanical technique[38–40]. Theoretical approaches[41–47], i.e. computational fluid dynamic, as well as experimental technique enables the researchers to improve their investigations in inaccessible conditions[48–55]. Thus these techniques are extensively used in engineering applications[55–61].

Hybrid techniques have been recently investigated as new approach for the drag and heat reduction on the nose cone flying at hypersonic speed[62,63]. In this methodology, spike is joint with either fluidic and energy methods to improve the performance of classical technique of mechanical methods[64–67]. Although this approach seems very efficient, it is not considered as practical method yet. In fact, the usage of either fluidic and energy device for thermal load reduction is done in the laboratory and no real practical applications of this method was not reported. Since this hybrid method was new method, limited resources and articles have been presented in this topic.

In this research, the usage of lateral jet for the cooling of the nose cone with multi-row disk (MRD) at high-speed flight is fully investigated (Fig. 1). The influence of jet location and condition on the cooling of the nose cone is investigated by the computational method. The highly compressible flow around the MRD blunt body is simulated and comprehensive flow analysis are presented to find the effective terms for thermal load management of the nose cone. The influence of coolant gas type is investigated by comparing carbon dioxide and helium jet in this investigation.

Governing equation and numerical method

This study applied RANS equations for modeling of the compressible flow near the nose cone with MRD device[68]. SST turbulence model is applied in the simulation of highly turbulent flow around the nose cone[69]. The flow is assumed ideal gas and species transport equation is also applied since the secondary gases of helium and CO_2 are used for the cooling in this hybrid technique. Computational fluid dynamic is applied for the simulation of flow around the nose while the coolant gas is released. This technique is popular for simulation of fluid in engineering problems[70,71]. The details of the main governing equations have extensively presented and explained in the previous articles and readers are referred to these resources[72,73].

Applied boundary condition related to the selected model is demonstrated in Fig. 2. Inflow is pressure farfield with M = 5.0, Pinf-2550 and Tinf = 221 K. Helium and carbon dioxide are chosen for as coolant jets with sonic condition at Ts = 300 K. Pressure outlet is extrapolated from the results of inside domain. The spike and main body is assumed wall with constant temperature of 300 K. The length of spike is equal to diameter of the main body[60].

Grid study as the main step for the computational fluid dynamic are done by producing different grids for our models. The number of grid in three directions are change to find optimum model in which results are independent from grid. Figure 3 demonstrated the schematic of produced grid for our model. Structured grid is used since it has more accuracy in the finite volume based approach. Table 1 presented details of grid studies. For grid independency analysis, four grid resolutions are generated and simulated in the first step. Comparison of the heat load on the main body are done for produced grids (Table 1) and it is found that fine grid with 1,628,000 cells.

Results and discussion

The comparison of experimental and numerical data with our results is done to perform validation. This step is important since it approves the correctness of applied method for the simulation of the chosen case. As presented in ref.[74], the variation of normalized pressure along the nose agrees reasonably with other methods. The deviation of the archived results from other techniques is not more than 8% in the simple nose cone at supersonic flow.

Streamline and coolant distribution for three lateral jets located on the stem of the spike are displayed in Fig. 4. The deflection of the main stream and the diffusion mechanism of Helium and CO_2 jet in these configurations are noticed in these models. The main effects of these jet locations are on the deflection of main stream while the
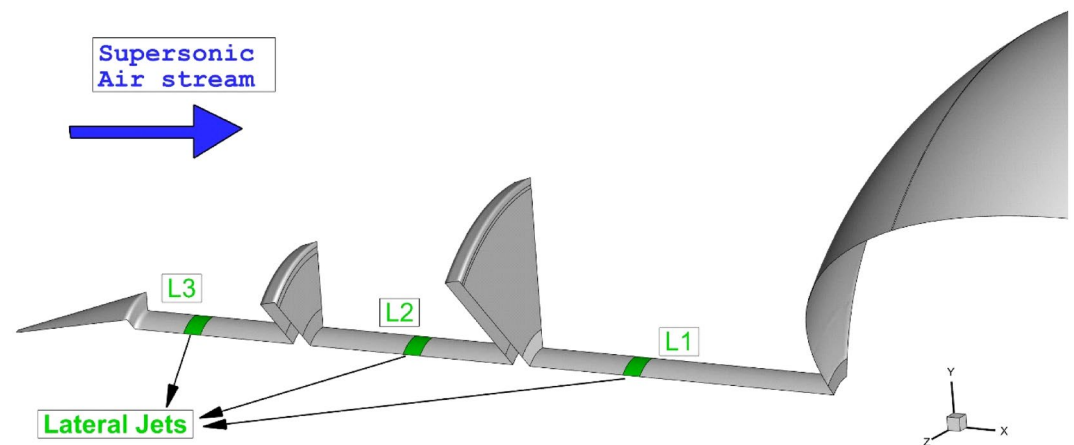

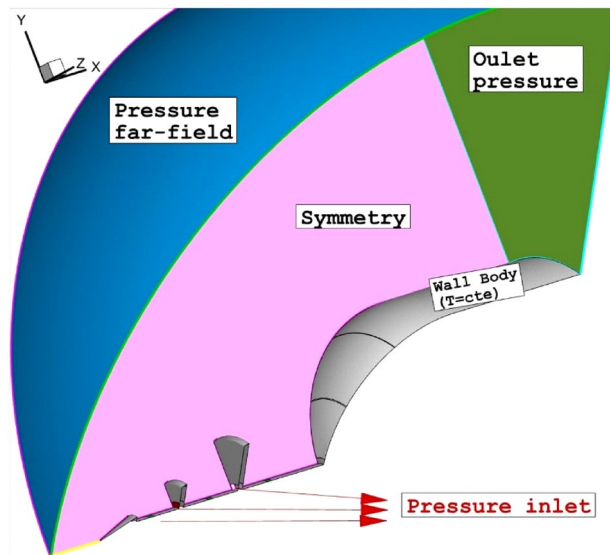**Figure 1.** Selected model with proposed injection system.
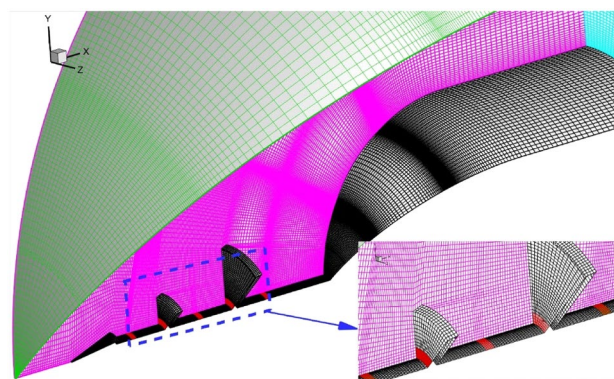
Figure 2. Applied boundary condition.

Figure 3. Grid production.

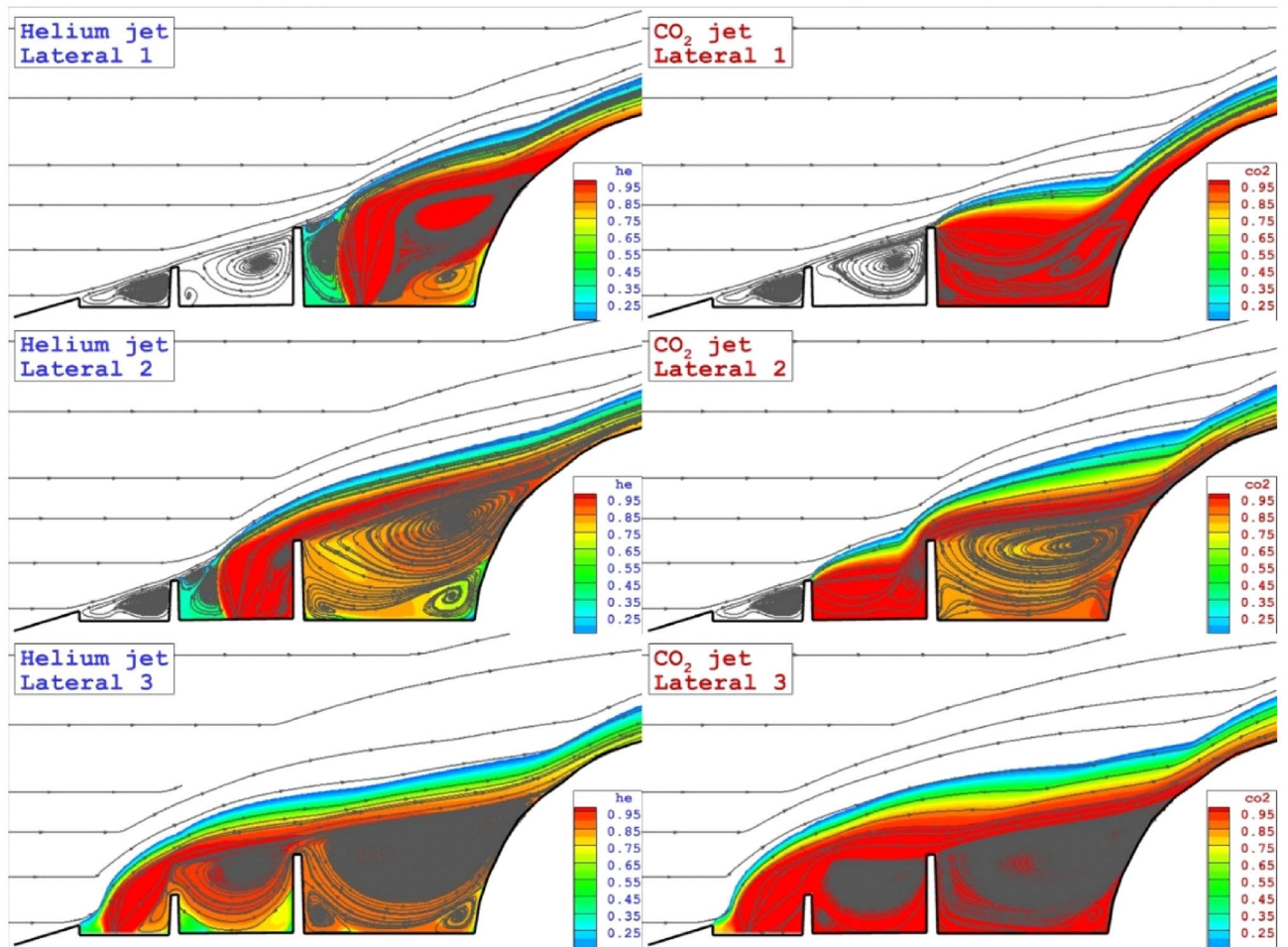| Model	Grid number	Average Stanton numb. on blunt cone ($\theta = 30$)	Average Stanton on numb. blunt cone ($\theta = 60$)
Coarse grid	680,000	0.00212	0.00618
Normal grid	960,000	0.00245	0.00637
Fine grid	1,320,000	0.00251	0.00651
Very fine grid	1,680,000	0.00253	0.00653

Table 1. Grid details.

Figure 4. Flow stream and concentration of the different lateral coolant injection systems.

circulation regime in these model is almost identical. Due to high penetration rate of helium, this gas deflects the bow shock with higher angles.

The feature of the shock interactions for lateral injection system are demonstrated in Fig. 5. The main difference on the jet location on the spike is related to the interaction of the separation shock with barrel shock of coolant jet. In fact, this interaction results in deflection of the bow shock and limited the interaction of the separation shock to the main body. As jet location move to the tip of the spike, the angle of the bow shock becomes more and separation layer did not touch the main body. Therefore, the heat transfer decreases on the main body.
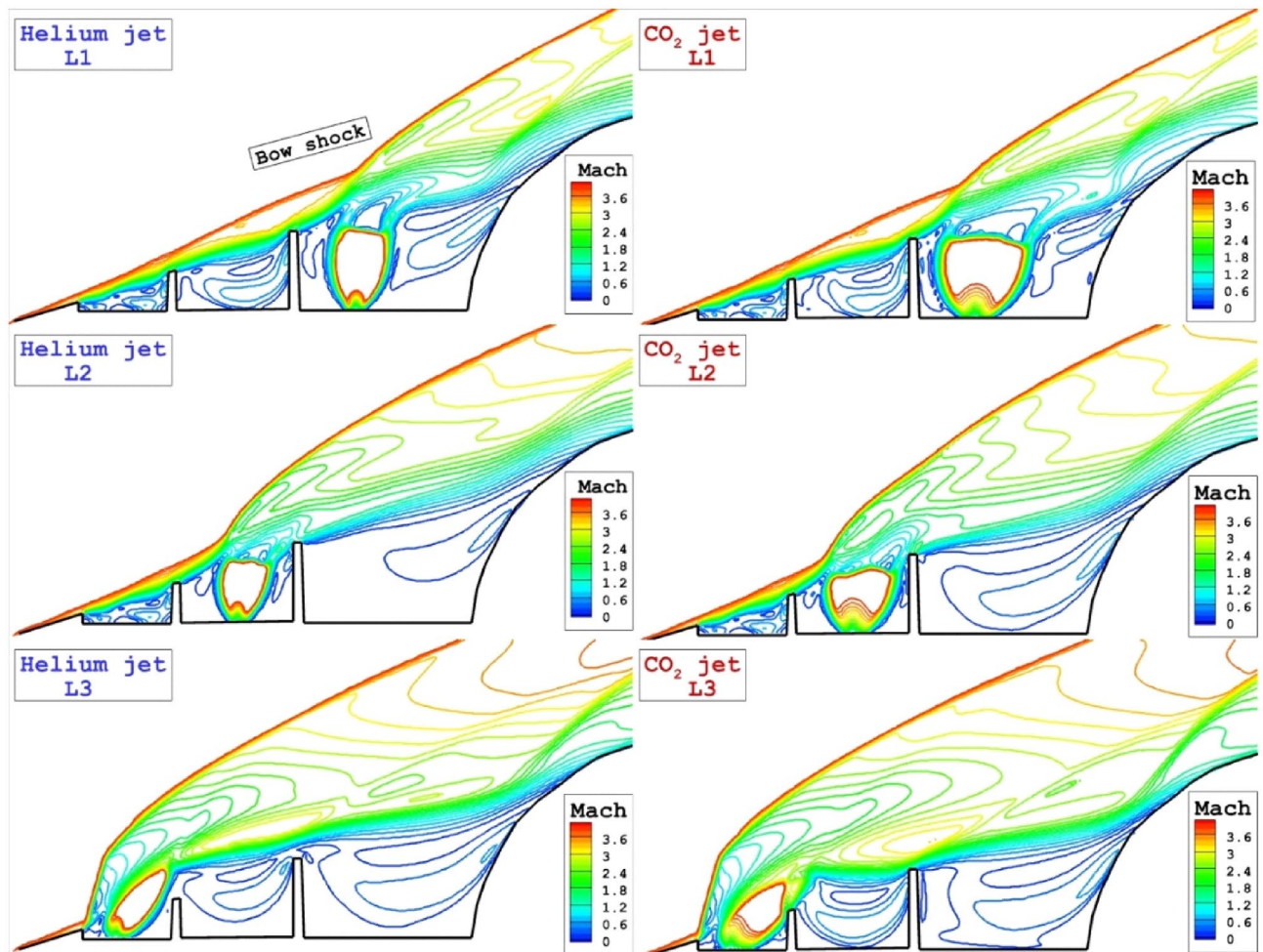
Figure 5. Influence of the different lateral coolant injection systems on shock interactions.

The main difference of these coolant jet is associated with the shape and size of barrel shock and their effects on the bow shock is almost identical.

To evaluate the strength of bow and barrel shocks, Fig. 6 demonstrates the temperature contour on the midplane for different lateral injection systems. When the lateral injection occurs in the vicinity of the main body, the hot region is nearby the tip of disks where the interaction of the bow shock with disk results in the high entropy region. As coolant injection move to the tip of the spike, the temperature region become restricted between barrel shock and the bow shock and this confirms the high power of bow shock. It is also found that the strength of deflection shock for helium jet is less than that of CO_2 jet. Besides, as the coolant jet moves to the main body, more portion of the body is under impacts of the cool fluid.
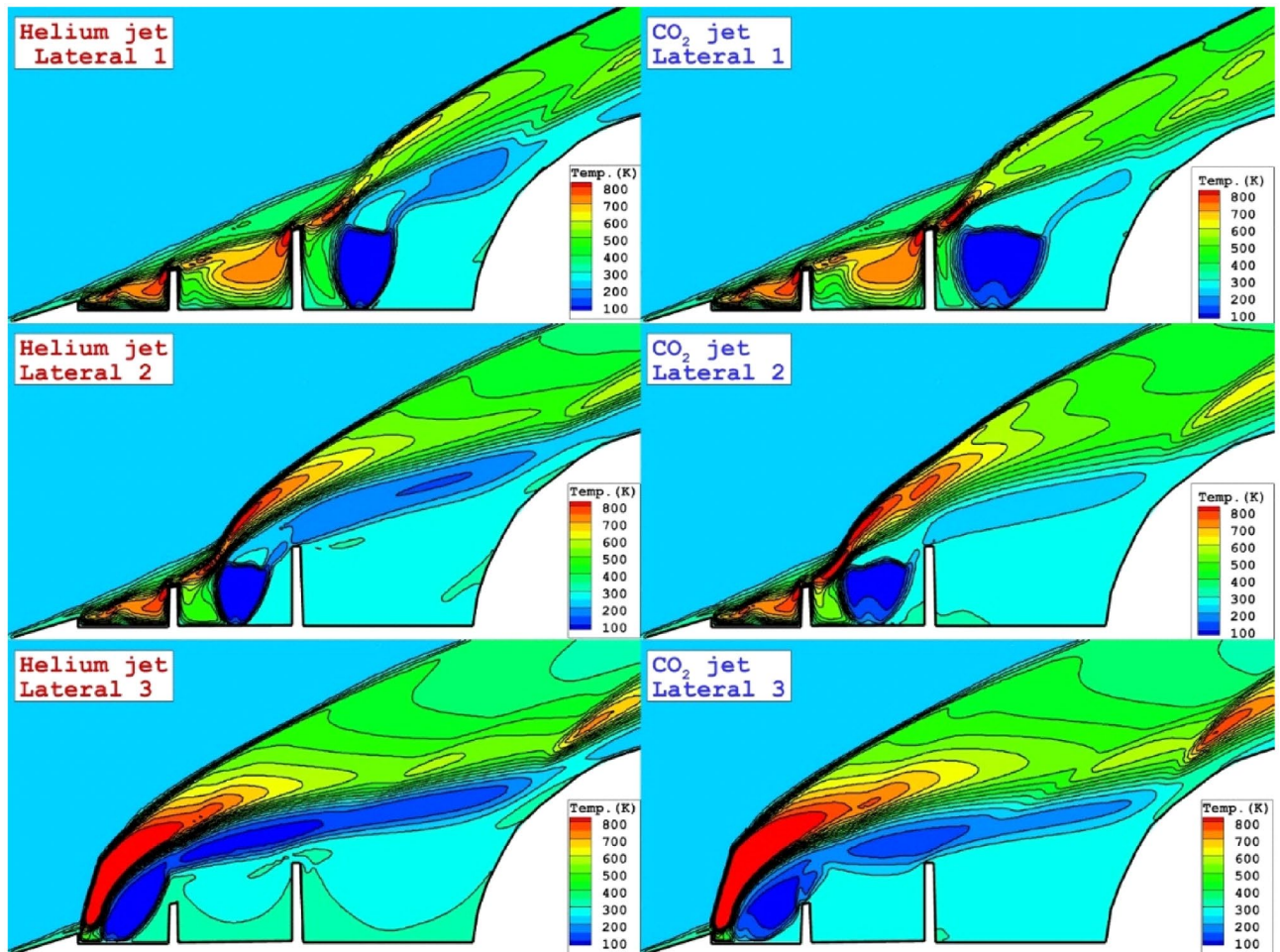
Figure 6. temperature distributions nearby the main body for the different lateral coolant injection systems.

Figure 7 illustrates the three-dimensional feature of the coolant layer to disclose the diffusion of these two gases in different lateral injection systems. Based on the achieved contour, the diffusion of the helium into the main bow shock cases the fluctuation and a segment of coolant diverted into the main body of the nose cone. This effect is noticed on the heat transfer rate displayed in Fig. 8. The heat transfer rate on the disk and main body indicates the diffusion mechanism of the coolant and its effects on the heat load of the nose and disk. As expected, high heat transfer rate occurs on the tip of the disk and this is because of shock deflection. Effects of coolant location is also noticed on the heat transfer of the main body.

Figure 9 demonstrates the effect of the different lateral coolant injection systems on the total heat load reduction on the main body and spike assembly. Obtained data indicates that the injection of CO_2 jet is more efficient than Helium for cooling of the body and spike assembly. In fact, this is due to the shield effects of the CO_2 gas since it has lower diffusivity than helium.
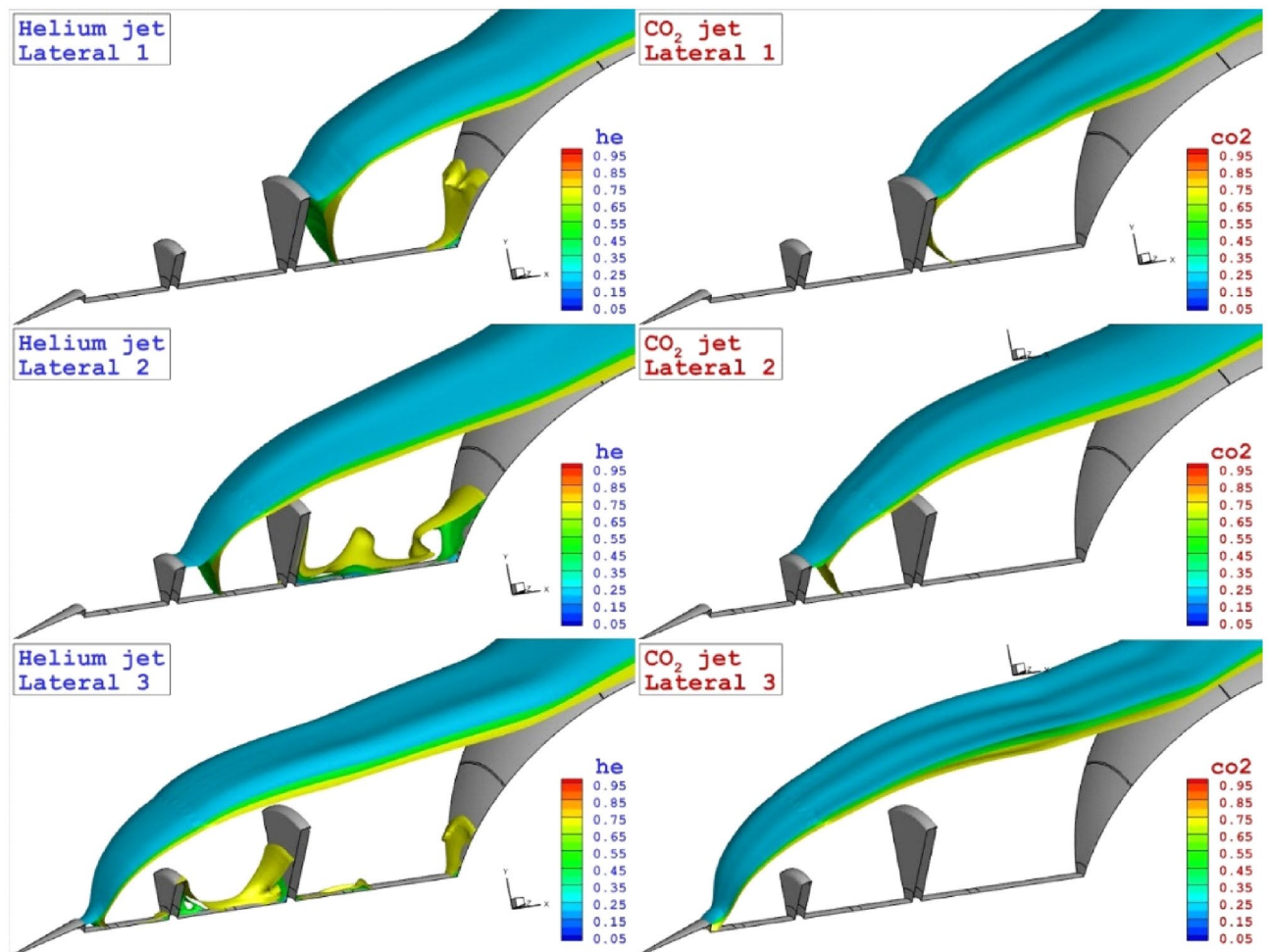
Figure 7. 3-D feature of the different lateral coolant injection systems.

Conclusion

This study tries to investigate the importance of the lateral jet for the thermal management of the nose cone with MRD flying at hypersonic flow. Three-dimensional model is used for the investigation of the flow and heat transfer near the nose cone and spike assembly. Flow analysis and coolant gas distribution are compared for two coolant gas types of helium and carbon dioxide. The influence of the coolant gas on the compression shock and bow shock near spike and main body. Mechanism of cooling in different jet locations is also investigated to achieve the optimum configuration for the thermal load reduction of the nose cone. Our results show that deflation of the main blow shock by the coolant jet near the spike tip has great impacts on the reduction of aerodynamic heating.
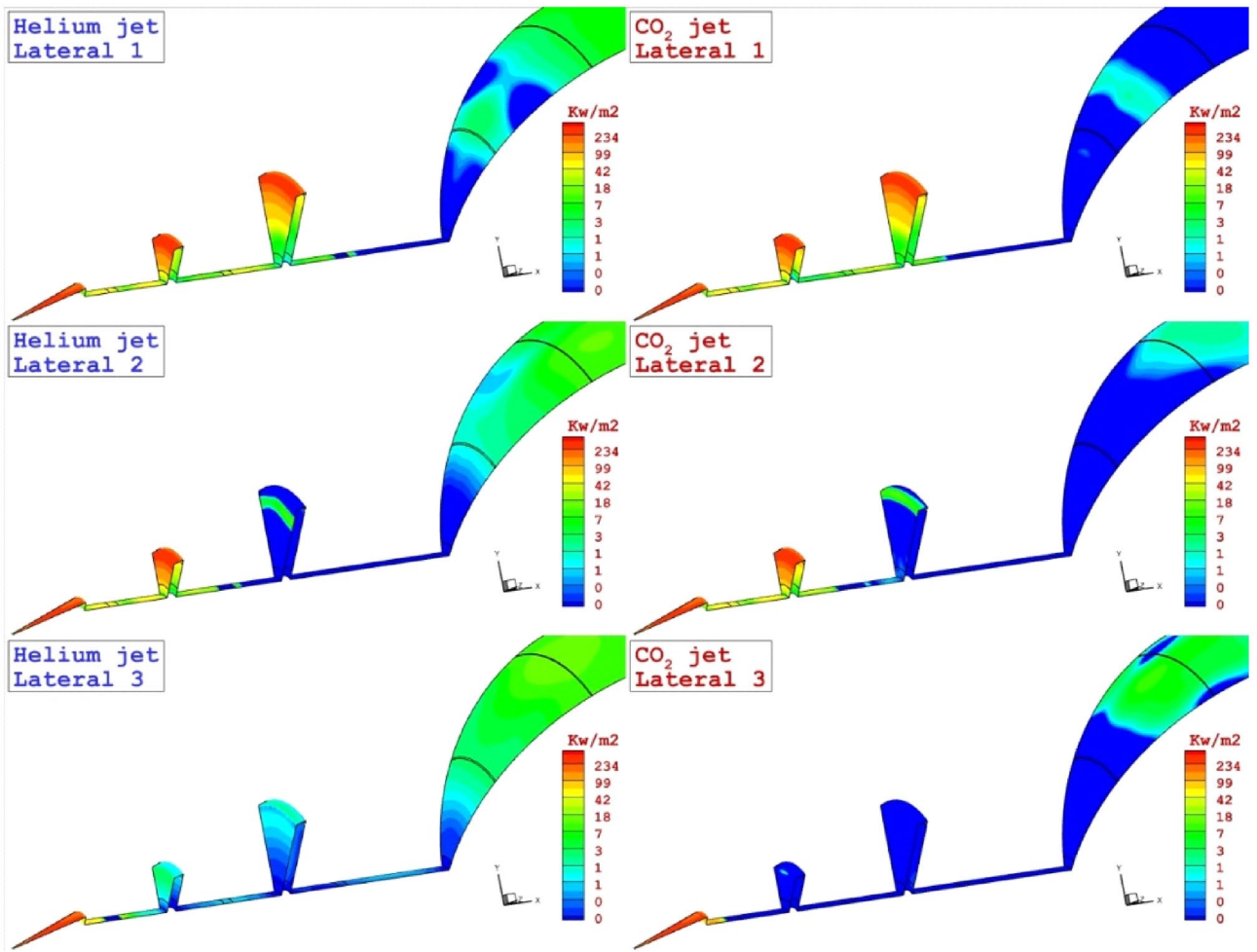
Figure 8. Heat transfer rate on the main body and disk of the different lateral coolant injection systems.
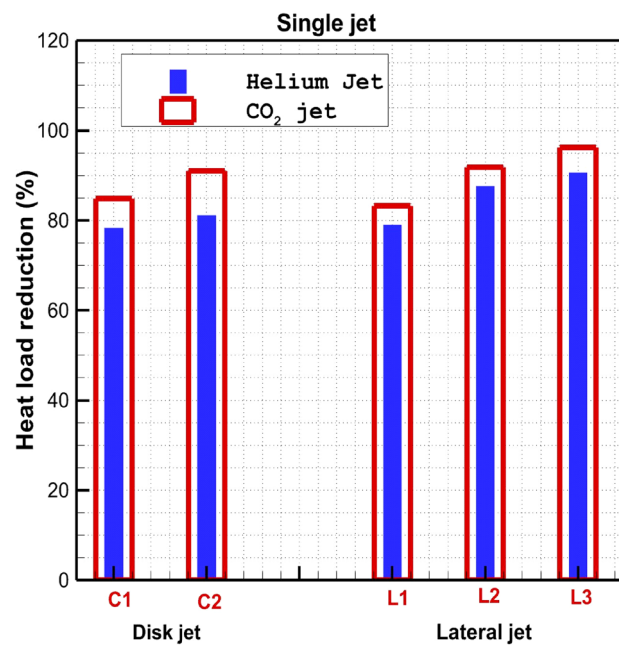

Figure 9. Comparison of heat load reduction of the different lateral coolant injection systems.

Data availability

The datasets used and/or analysed during the current study available from the corresponding author on reasonable request.

References

1. Du, S. *et al.* Effect of fuel jet arrangement on the mixing rate inside trapezoidal cavity flame holder at supersonic flow. *Int. J. Hydrogen Energy* **44**(39), 22231–22239 (2019).
2. Ji, C. *et al.* Design exploration on the drag reduction and thermal protection over a blunted waverider with multiple opposing jets. *Aerosp. Sci. Technol.* **124**, 107519 (2022).
3. Pish, F. *et al.* Computational study of the cavity flow over sharp nose cone in supersonic flow. *Int. J. Mod. Phys. C* **31**(06), 2050079 (2020).
4. Li, Z., Moradi, R., Marashi, S. M., Babazadeh, H. & Choubey, G. Influence of backward-facing step on the mixing efficiency of multi microjets at supersonic flow. *Acta Astronaut.* **175**, 37–44 (2020).
5. Du, Z. B. *et al.* Parametric study on mixing augmentation mechanism induced by cantilevered ramp injectors in a shock-induced combustion ramjet engine. *Aerosp. Sci. Technol.* **108**, 106413 (2021).
6. Gerdroodbary, M. B. & Hosseinalipour, S. M. Numerical simulation of hypersonic flow over highly blunted cones with spike. *Acta Astronaut.* **67**(1–2), 180–193 (2010).
7. Gerdroodbary, M. B. *Aerodynamic Heating in Supersonic and Hypersonic Flows: Advanced Techniques for Drag and Aero-Heating Reduction* (Elsevier, 2022).
8. Liu, X. *et al.* Computational study of the multi hydrogen jets in presence of the upstream step in a Ma = 4 supersonic flow. *Int. J. Hydrogen Energy* **45**(55), 31118–31129 (2020).
9. Barzegar Gerdroodbary, M., Moradi, R. & Babazadeh, H. Computational investigation of multi hydrogen jets at inclined supersonic flow. *Int. J. Energy Res* **45**(2), 1661–1672 (2021)
10. Gerdroodbary, M. B., Bishehsari, S., Hosseinalipour, S. M. & Sedighi, K. Transient analysis of counterflowing jet over highly blunt cone in hypersonic flow. *Acta Astronaut.* **73**, 38–48 (2012).
11. Pish, F., Hassanvand, A., BarzegarGerdroodbary, M. & Noori, S. Viscous equilibrium analysis of heat transfer on blunted cone at hypersonic flow. *Case Stud. Therm. Eng.* **14**, 100464 (2019).
12. BarzegarGerdroodbary, M. Numerical analysis on cooling performance of counterflowing jet over aerodisked blunt body. *Shock Waves* **24**(5), 537–543 (2014).
13. Choubey, G. *et al.* Recent advances in cavity-based scramjet engine—A brief review. *Int. J. Hydrogen Energy* **44**(26), 13895–13909 (2019).
14. Feszty, D., Badcock, K. J. & Richards, B. E. Driving mechanisms of high-speed unsteady spiked body flows, part 2: Oscillation mode. *AIAA J.* **42**(1), 107–113 (2004).
15. Dong, M. Z., Liao, J., Choubey, G. & Huang, W. Influence of the secondary flow control on the transverse gaseous injection flow field properties in a supersonic flow. *Acta Astronaut.* **165**, 150–157 (2019).
16. Liu, X. *et al.* Effect of strut angle on performance of hydrogen multi-jets inside the cavity at combustion chamber. *Int. J. Hydrogen Energy* **45**(55), 31179–31187 (2020).
17. BarzegarGerdroodbary, M. *Scramjets: Fuel Mixing and Injection Systems* 1–220 (Elsevier Ltd., 2020).
18. Edalatpour, A., Hassanvand, A., Gerdroodbary, M. B., Moradi, R. & Amini, Y. Injection of multi hydrogen jets within cavity flameholder at supersonic flow. *Int. J. Hydrogen Energy* **44**(26), 13923–13931 (2019).
19. Hassanvand, A., Gerdroodbary, M. B. & Abazari, A. M. Injection of hydrogen sonic multi-jet on inclined surface at supersonic flow. *Int. J. Mod. Phys. C* **32**(03), 2150043 (2021).
20. Jiang, Y. *et al.* Effect of cavity back height on mixing efficiency of hydrogen multi-jets at supersonic combustion chamber. *Int. J. Hydrogen Energy* **45**, 27828–27836 (2020).
21. Sun, C., Gerdroodbary, M. B., Abazari, A. M., Hosseini, S. & Li, Z. Mixing efficiency of hydrogen multijet through backward-facing steps at supersonic flow. *Int. J. Hydrogen Energy* **46**, 16075–16085 (2021).
22. Liu, X. *et al.* Numerical simulation of the hydrogen mixing in downstream of lobe strut at supersonic flow. *Int. J. Hydrogen Energy* **45**, 25438–25451 (2020).
23. Hassanvand, A., Saei Moghaddam, M., BarzegarGerdroodbary, M. & Amini, Y. Analytical study of heat and mass transfer in axisymmetric unsteady flow by ADM. *J. Comput. Appl. Res. Mech. Eng.* **11**(1), 151–163 (2021).
24. Jiang, Y. *et al.* Effect of free stream angle on mixing performance of hydrogen multi-jets in supersonic combustion chamber. *Int. J. Hydrogen Energy* **45**(46), 25426–25437 (2020).
25. Amini, Y. & Nasr Esfahany, M. CFD simulation of the structured packings: A review. *Sep. Sci. Technol.* **54**(15), 2536–2554 (2019).
26. Li, Z. *et al.* Computational investigation of multi-cavity fuel injection on hydrogen mixing at supersonic combustion chamber. *Int. J. Hydrogen Energy* **45**(15), 9077–9087 (2020).
27. Zhang, Y., Gerdroodbary, M. B., Hosseini, S., Abazari, A. M. & Li, Z. Effect of hybrid coaxial air and hydrogen jets on fuel mixing at supersonic crossflow. *Int. J. Hydrogen Energy* **46**(29), 16048–16062 (2021).
28. Li, Z. *et al.* The influence of the wedge shock generator on the vortex structure within the trapezoidal cavity at supersonic flow. *Aerosp. Sci. Technol.* **98**, 105695 (2020).
29. Zhu, L., Chen, X., Li, Y., Musa, O. & Zhou, C. Investigation of drag and heat reduction induced by a novel combinational lateral jet and spike concept in supersonic flows based on conjugate heat transfer approach. *Acta Astronaut.* **142**, 300–313 (2018).
30. Gerdroodbary, M. B., Goudarzi, A. M., Imani, M., Sedighi, K. & Ganji, D. D. Influence of opposing jet on an aerodisk nose cone at hypersonic flow. In *Engineering Systems Design and Analysis*, vol. 45837, V001T13A007. (American Society of Mechanical Engineers, 2014).
31. Manh, T. D., Nam, N. D., Gerdroodbary, M. B., Babazadeh, H. & Moradi, R. Numerical simulation of mixing of hydrogen jet at supersonic cross flow in presence of upstream wavy wall. *Int. J. Hydrogen Energy* **45**(1), 1096–1106 (2020).
32. Li, Y., Gerdroodbary, M. B., Moradi, R. & Babazadeh, H. The influence of the sinusoidal shock generator on the mixing rate of multi hydrogen jets at supersonic flow. *Aerosp. Sci. Technol.* **96**, 105579 (2020).
33. Isanejad, M. & Fallah, K. Numerical study of droplet breakup in an asymmetric T-junction microchannel with different cross-section ratios. *Int. J. Mod. Phys. C* **33**(02), 2250023 (2022).
34. Fallah, K. & Fattahi, E. Splitting of droplet with different sizes inside a symmetric T-junction microchannel using an electric field. *Sci. Rep.* **12**(1), 1–12 (2022).
35. Fallah, K., Rahni, M. T., Mohammadzadeh, A. & Najafi, M. Drop formation in cross-junction microchannel, using lattice Boltzmann method. *Therm. Sci.* **22**(2), 909–919 (2018).
36. Allahyari, S. *et al.* Investigating the effects of nanoparticles mean diameter on laminar mixed convection of a nanofluid through an inclined tube with circumferentially nonuniform heat flux. *J. Eng. Thermophys.* **25**(4), 563–575 (2016).

37. Ahmadi Asoor, A. A., Valipour, P. & Ghasemi., S. E. Investigation on vibration of single-walled carbon nanotubes by variational iteration method. *Applied Nanoscience* **6**, 243–249 (2016)

38. Valipour, P., & Ghasemi, S. E. Numerical investigation of MHD water-based nanofluids flow in porous medium caused by shrinking permeable sheet. *J. Braz. Soc. Mech. Sci. Eng.* **38**, 859–868 (2016)

39. Amini, Y., Gerdroodbary, M. B., Pishvaie, M. R., Moradi, R. & Monfared, S. M. Optimal control of batch cooling crystallizers by using genetic algorithm. *Case Stud. Therm. Eng.* **8**, 300–310 (2016).

40. Amini, Y., Mokhtari, M., Haghshenasfard, M. & Gerdroodbary, M. B. Heat transfer of swirling impinging jets ejected from nozzles with twisted tapes utilizing CFD technique. *Case Stud. Therm. Eng.* **6**, 104–115 (2015).

41. Xue, B. *et al.* An AuNPs/mesoporous NiO/nickel foam nanocomposite as a miniaturized electrode for heavy metal detection in groundwater. *Engineering* https://doi.org/10.1016/j.eng.2022.06.005 (2022).

42. Li, P., Yang, M. & Wu, Q. Confidence interval based distributionally robust real-time economic dispatch approach considering wind power accommodation risk. *IEEE Trans. Sustain. Energy* **12**(1), 58–69 (2021).

43. Si, Z., Yang, M., Yu, Y. & Ding, T. Photovoltaic power forecast based on satellite images considering effects of solar position. *Appl. Energy* **302**, 117514. https://doi.org/10.1016/j.apenergy.2021.117514 (2021).

44. Wang, M., Yang, M., Fang, Z., Wang, M. & Wu, Q. A practical feeder planning model for urban distribution system. *IEEE Trans. Power Syst.* https://doi.org/10.1109/TPWRS.2022.3170933 (2022).

45. Cheng, F., Liang, H., Niu, B., Zhao, N. & Zhao, X. Adaptive neural self-triggered bipartite secure control for nonlinear MASs subject to DoS attacks. *Inf. Sci.* **631**, 256–270 (2023).

46. Tang, F., Wang, H., Chang, X. H., Zhang, L. & Alharbi, K. H. Dynamic event-triggered control for discrete-time nonlinear Markov jump systems using policy iteration-based adaptive dynamic programming. *Nonlinear Anal. Hybrid Syst.* **49**, 101338 (2023).

47. Cheng, Y., Niu, B., Zhao, X., Zong, G. & Ahmad, A. M. Event-triggered adaptive decentralized control of interconnected nonlinear systems with Bouc-Wen hysteresis input. *Int. J. Syst. Sci.* https://doi.org/10.1080/00207721.2023.2169845 (2023).

48. Zhang, H., Zou, Q., Ju, Y., Song, C. & Chen, D. Distance-based support vector machine to predict DNA N6-methyladine modification. *Curr. Bioinform.* **17**(5), 473–482 (2022).

49. Ghazanfari, V., Imani, M., Shadman, M. M., Zahakifar, F. & Amini, Y. Numerical study on the thermal performance of the shell and tube heat exchanger using twisted tubes and Al_2O_3 nanoparticles. *Prog. Nucl. Energy* **155**, 104526 (2023).

50. Sadeghi, A., Amini, Y., Saidi, M. H. & Chakraborty, S. Numerical modeling of surface reaction kinetics in electrokinetically actuated microfluidic devices. *Anal. Chim. Acta* **838**, 64–75 (2014).

51. Xie, L. *et al.* Self-feature-based point cloud registration method with a novel convolutional Siamese point net for optical measurement of blade profile. *Mech. Syst. Signal Process.* **178**, 109243. https://doi.org/10.1016/j.ymssp.2022.109243 (2022).

52. Yin, M., Zhu, Y., Yin, G., Fu, G. & Xie, L. Deep feature interaction network for point cloud registration, with applications to optical measurement of blade profiles. *IEEE Trans. Ind. Inform.* https://doi.org/10.1109/TII.2022.3220889 (2022).

53. Yan, A. *et al.* Design of double-upset recoverable and transient-pulse filterable latches for low-power and low-orbit aerospace applications. *IEEE Trans. Aerosp. Electron. Syst.* **56**(5), 3931–3940. https://doi.org/10.1109/TAES.2020.2982341 (2020).

54. Rong, G. *et al.* Investigation of counter-rotating shock wave and wave direction control of hollow rotating detonation engine with Laval nozzle. *Phys. Fluids* **34**(5), 56104. https://doi.org/10.1063/5.0089207 (2022).

55. Li, H., Li, G. & Li, L. Comparative investigation on combustion characteristics of ADN-based liquid propellants in inert gas and oxidizing gas atmospheres with resistive ignition method. *Fuel* **334**, 126742. https://doi.org/10.1016/j.fuel.2022.126742 (2023).

56. Shao, Z., Zhai, Q., Han, Z. & Guan, X. A linear AC unit commitment formulation: An application of data-driven linear power flow model. *Int. J. Electr. Power Energy Syst.* **145**, 108673. https://doi.org/10.1016/j.ijepes.2022.108673 (2023).

57. Bai, X., Shi, H., Zhang, K., Zhang, X. & Wu, Y. Effect of the fit clearance between ceramic outer ring and steel pedestal on the sound radiation of full ceramic ball bearing system. *J. Sound Vib.* **529**, 116967. https://doi.org/10.1016/j.jsv.2022.116967 (2022).

58. Yang, C., Zhang, J. & Huang, Z. Numerical study on cavitation-vortex-noise correlation mechanism and dynamic mode decomposition of a hydrofoil. *Phys. Fluids* **34**(12), 125105. https://doi.org/10.1063/5.0128169 (2022).

59. Liu, L., Mei, Q. & Jia, W. A flexible diesel spray model for advanced injection strategy. *Fuel* **314**, 122784. https://doi.org/10.1016/j.fuel.2021.122784 (2022).

60. Zhu, L. *et al.* Novel combinational aerodisk and lateral jet concept for drag and heat reduction in hypersonic flows. *J. Aerosp. Eng.* **32**(1), 04018133 (2019).

61. Hassanvand, A., Gerdroodbary, M. B., Fallah, K. & Moradi, R. Effect of dual micro fuel jets on mixing performance of hydrogen in cavity flameholder at supersonic flow. *Int. J. Hydrogen Energy* **43**(20), 9829–9837 (2018).

62. Jiang, Y. *et al.* Influence of upstream strut on hydrogen fuel distribution inside the supersonic combustion chamber. *Int. J. Hydrogen Energy* **45**, 22032–22040 (2020).

63. Li, Z. *et al.* Mixing enhancement of multi hydrogen jets through the cavity flameholder with extended pylon. *Acta Astronaut.* **175**, 300–307 (2020).

64. Pish, F., Moradi, R., Edalatpour, A. & Gerdroodbary, M. B. The effect of coolant injection from the tip of spike on aerodynamic heating of nose cone at supersonic flow. *Acta Astronaut.* **154**, 52–60 (2019).

65. Moradi, R., Mahyari, A., Gerdroodbary, M. B., Abdollahi, A. & Amini, Y. Shape effect of cavity flameholder on mixing zone of hydrogen jet at supersonic flow. *Int. J. Hydrogen Energy* **43**(33), 16364–16372 (2018).

66. Moradi, R., Mosavat, M., Gerdroodbary, M. B., Abdollahi, A. & Amini, Y. The influence of coolant jet direction on heat reduction on the nose cone with Aerodome at supersonic flow. *Acta Astronaut.* **151**, 487–493 (2018).

67. Qin, Q., Xu, J. & Guo, S. Fluid–thermal analysis of aerodynamic heating over spiked blunt body configurations. *Acta Astronaut.* **132**, 230–242 (2017).

68. Li, Z., Gerdroodbary, M. B., Moradi, R., Manh, T. D. & Babazadeh, H. Effect of inclined block on fuel mixing of multi hydrogen jets in scramjet engine. *Aerosp. Sci. Technol.* **105**, 106035 (2020).

69. Menter, F. R. Two-equation eddy-viscosity turbulence models for engineering applications. *AIAA J.* **32**(8), 1598–1605 (1994).

70. Sheidani, A., Salavatidezfouli, S. & Schito, P. Study on the effect of raindrops on the dynamic stall of a NACA-0012 airfoil. *J Braz. Soc. Mech. Sci. Eng.* **44**, 203. https://doi.org/10.1007/s40430-022-03498-8 (2022).

71. Bakhshaei, K., MoradiMaryamnegari, H., SalavatiDezfouli, S., Khoshnood, A. M. & Fathali, M. Multi-physics simulation of an insect with flapping wings. *Proc. Inst. Mech. Eng. Part G J. Aerospace Eng.* **235**(10), 1318–1339 (2021).

72. Jiang, Y., Hajivand, M., Sadeghi, H., Gerdroodbary, M. B. & Li, Z. Influence of trapezoidal lobe strut on fuel mixing and combustion in supersonic combustion chamber. *Aerosp. Sci. Technol.* **116**, 106841 (2021).

73. Dechaumphai, P., Thornton, E. A. & Weiting, A. R. Flow-thermal structural study of aerodynamically heated leading edges. *J. Spacecraft Rockets* **26**(4), 201–209 (1989).

74. Iranmanesh, R. *et al.* Numerical investigation of compressible flow around nose cone with multi-row disk and multi coolant jets. *Sci. Rep.* **13**, 787. https://doi.org/10.1038/s41598-023-28127-9 (2023).

Author contributions

K.F. and A.A. wrote the main manuscript text and M.S. and G.C. prepared figures. Y.S. and Q.C. prepared revisions and H.Y. reviewed manuscript and correct english writing. All authors reviewed the manuscript.

Competing interests

The authors declare no competing interests.

Additional information

Correspondence and requests for materials should be addressed to Y.S. or K.F.

Reprints and permissions information is available at www.nature.com/reprints.

Publisher's note Springer Nature remains neutral with regard to jurisdictional claims in published maps and institutional affiliations.